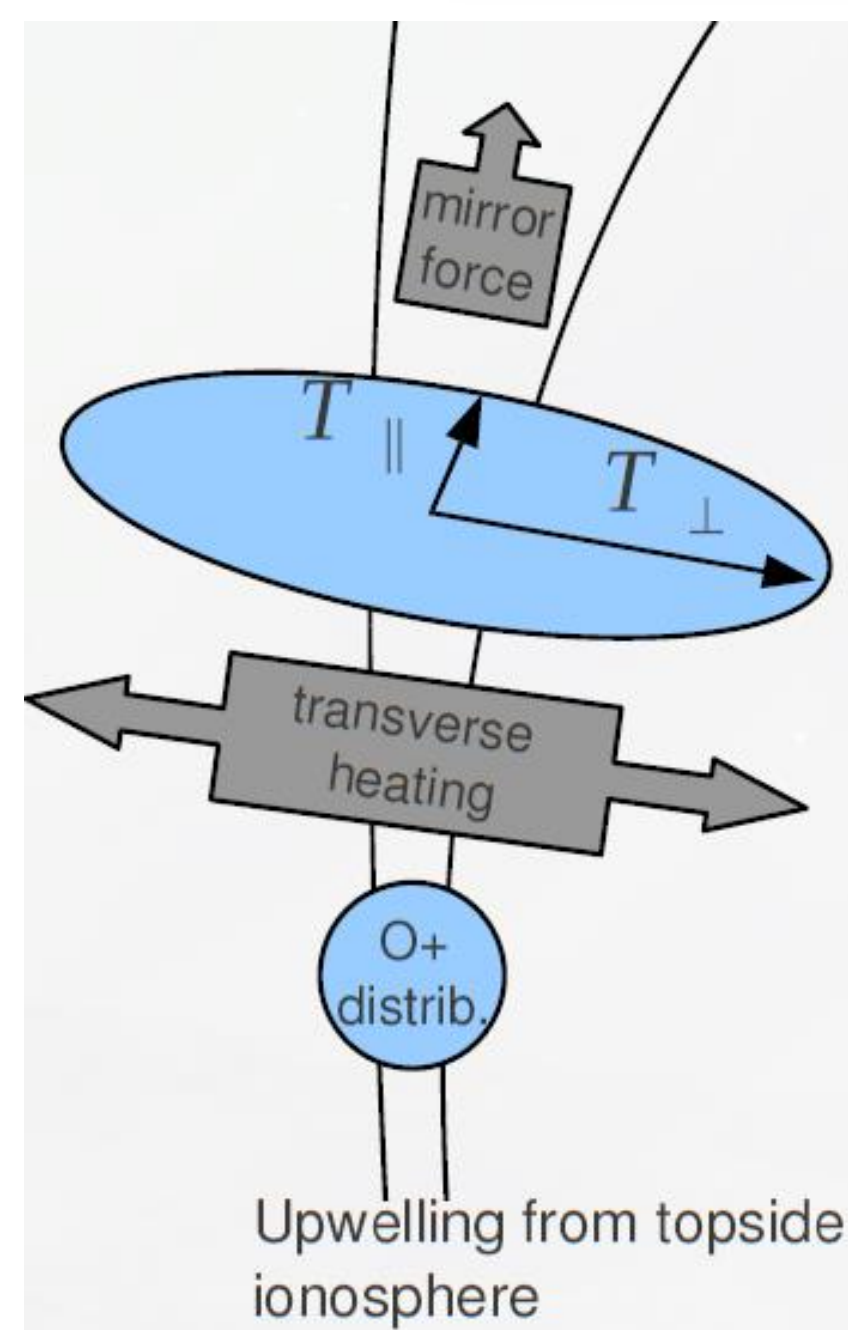


## Introduction



- Significant amounts of ionospheric plasma can be transported to high altitudes (ion upflow) in response to a variety of plasma heating and uplifting processes.
- Strong DC electric fields frictionally heat the ion population resulting in anisotropic increases in ion temperature that cause large pressure gradients which push the ions outward and upward.
- Soft electron precipitation heats ambient, F-region ionospheric electrons creating electron pressure gradients which in turn increase the ambipolar electric field, driving ion upflows.
- Once ions have been lifted to high altitudes, transverse ion acceleration by broadband ELF waves can give the upflowing ions sufficient energy to escape into the magnetosphere (ion outflow).

## Anisotropic Modeling of the Ionosphere

The 2D anisotropic fluid ionospheric model, GEMINI-TIA, is based on a truncated 16-moment description, and solves the time-dependent, nonlinear equations of conservation of mass, momentum, parallel and perpendicular energy [Barakat and Schunk 1982a] for seven ion species:

$$\frac{\partial \rho_s}{\partial t} + \nabla \cdot (\rho_s \mathbf{u}_s) = m_s P_s - L_s \rho_s$$

$$\frac{\partial \rho_s \mathbf{u}_s}{\partial t} \cdot \hat{\mathbf{e}}_{\parallel} + [\nabla \cdot (\rho_s \mathbf{u}_s \mathbf{u}_s)] \cdot \hat{\mathbf{e}}_{\parallel} = (\rho_s \mathbf{g}) \cdot \hat{\mathbf{e}}_{\parallel} - \nabla_{\parallel} p_{s,\parallel} + \left( \frac{\rho_s}{m_s} q_s \mathbf{E} \right) \cdot \hat{\mathbf{e}}_{\parallel} - (p_{s,\parallel} - p_{s,\perp}) \nabla \cdot \hat{\mathbf{e}}_{\parallel} + \frac{\delta M_s}{\delta t}$$

$$\frac{\partial p_{s,\parallel}}{\partial t} + \nabla \cdot (p_{s,\parallel} \mathbf{u}_s) = -2p_{s,\parallel} (\nabla_{\parallel} \cdot \mathbf{u}_s) - \nabla \cdot (h_{s,\parallel} \hat{\mathbf{e}}_{\parallel}) + 2h_{s,\perp} (\nabla \cdot \hat{\mathbf{e}}_{\parallel}) + \frac{\delta E_{s,\parallel}}{\delta t}$$

$$\frac{\partial p_{s,\perp}}{\partial t} + \nabla \cdot (p_{s,\perp} \mathbf{u}_s) = -p_{s,\perp} (\nabla_{\perp} \cdot \mathbf{u}_s) + \dot{W}_{s,\perp} - \nabla \cdot (h_{s,\perp} \hat{\mathbf{e}}_{\parallel}) - h_{s,\perp} (\nabla \cdot \hat{\mathbf{e}}_{\parallel}) + \frac{\delta E_{s,\perp}}{\delta t}$$

- System of equations is closed through an electrostatic treatment of the auroral currents:  $\nabla_{\perp} \cdot (\sigma_{\perp} \nabla_{\perp} \Phi) + \nabla_{\parallel} \cdot (\sigma_{\parallel} \nabla_{\parallel} \Phi) = \nabla_{\perp} \cdot (\sum_s n_s m_s v_{s,\perp} \cdot \mathbf{v}_{n,\perp})$  [Zettergren and Semeter 2012].
- The heat fluxes have been specified by 'equations of state':  $h_{s,\parallel,\perp} = -\frac{2}{3} \lambda_s \nabla_{\parallel,\perp} T_{s,\parallel,\perp} \cdot \hat{\mathbf{e}}_{\parallel}$
- Stress has been set to zero, a common assumption in models [c.f. Schunk 1975].
- Includes chemical interactions with the neutral atmosphere, photoionization, and electron impact ionization [Solomon and Qian 2005, Fang et al. 2008].
- All of the collision terms contain descriptions for both ion-ion and ion-neutral collisions [Blelly and Schunk 1993, Barakat and Schunk 1982a, Demars and Schunk 1979].
- The speed dependence of the collision cross sections is included as well [Gaimard et al. 1998].
- An ad hoc heating term is added to the model to encapsulate wave-particle interactions (cyclotron resonate heating),  $\dot{W}_{s,\perp} = 2m_s \left( \frac{\eta q_s^2}{4m_s^2} \right) |E_o|^2 \left( \frac{\omega_o}{\omega} \right)^\alpha$  [Zeng et al., 2006].

Since important temperature anisotropies, which can result from perpendicular DC electric fields and wave-particle interactions (e. g. in Figure 2), are not resolved in isotropic models and may result in overestimated ionospheric velocities and the amount of plasma supplied to higher altitudes (e.g. in Figure 1), the anisotropic model, GEMINI-TIA, was constructed to resolve these.

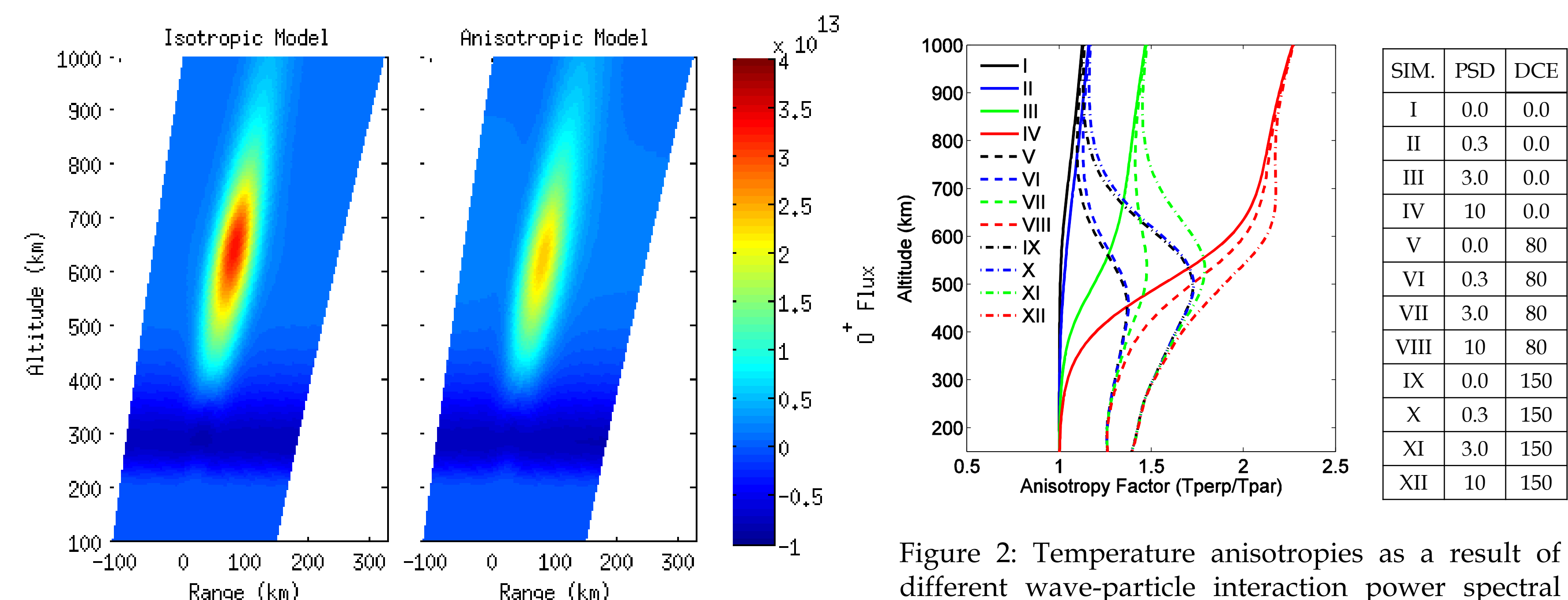


Figure 1: Comparing the O<sup>+</sup> particle flux between a 5-moment (isotropic) model and GEMINI-TIA, the 16-moment (anisotropic) model, after 100 s of a continuously applied DC electric field. Applied using a Gaussian distribution over the Range with a peak value of 80 mV/m.

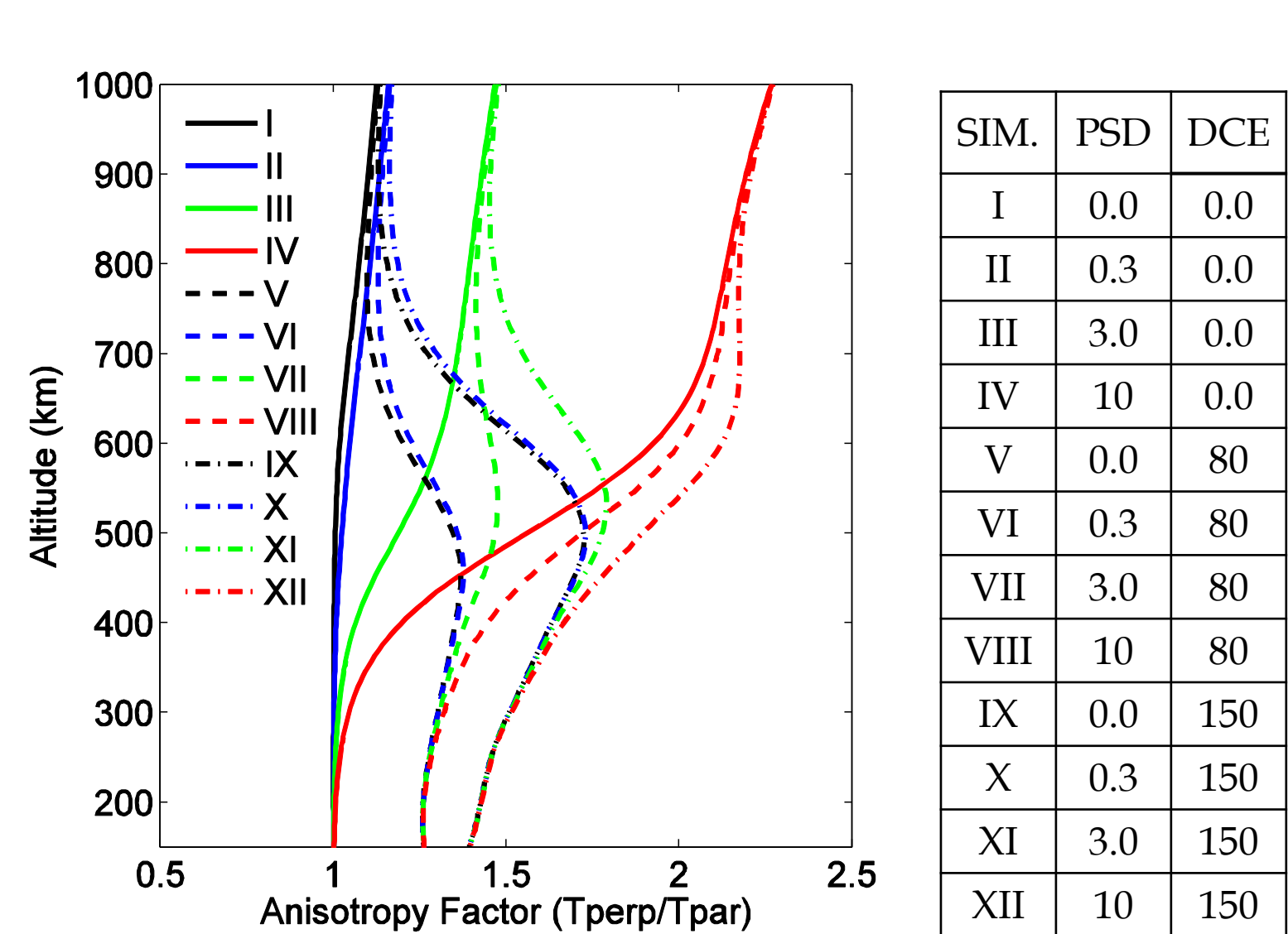


Figure 2: Temperature anisotropies as a result of different wave-particle interaction power spectral densities (PSD) [changes in color] and DC electric fields (DCE) [changes in line style] combinations after 30s of applied drivers. At lower altitudes collisional effects dampen wave-particle heating and DCE effects dominate.

## VISIONS Sounding Rocket Campaign

The VISIONS (VISualizing Ion Outflow via Neutral atom imaging during a Substorm) sounding rocket was launched on the 7<sup>th</sup> of February 2013 at 821 UT from Poker Flat, AK into the expansion phase of an auroral substorm. During the flight, VISIONS flew through several regions of auroral activity observing transversely flowing ions coincident with DC electric fields. Constrained by in-situ measurements, GEMINI-TIA is used to generate greater contextual detail of the state of the ionosphere during this flight.

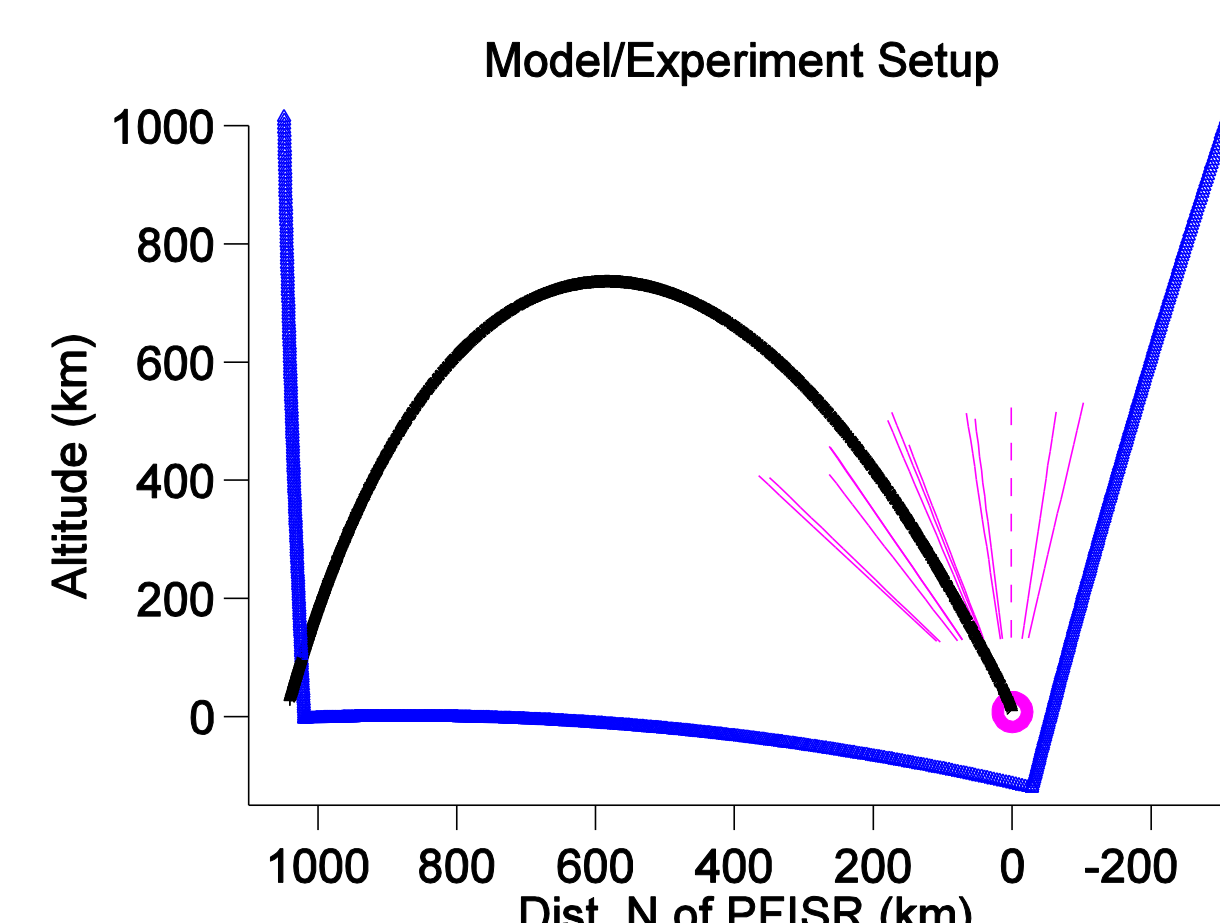
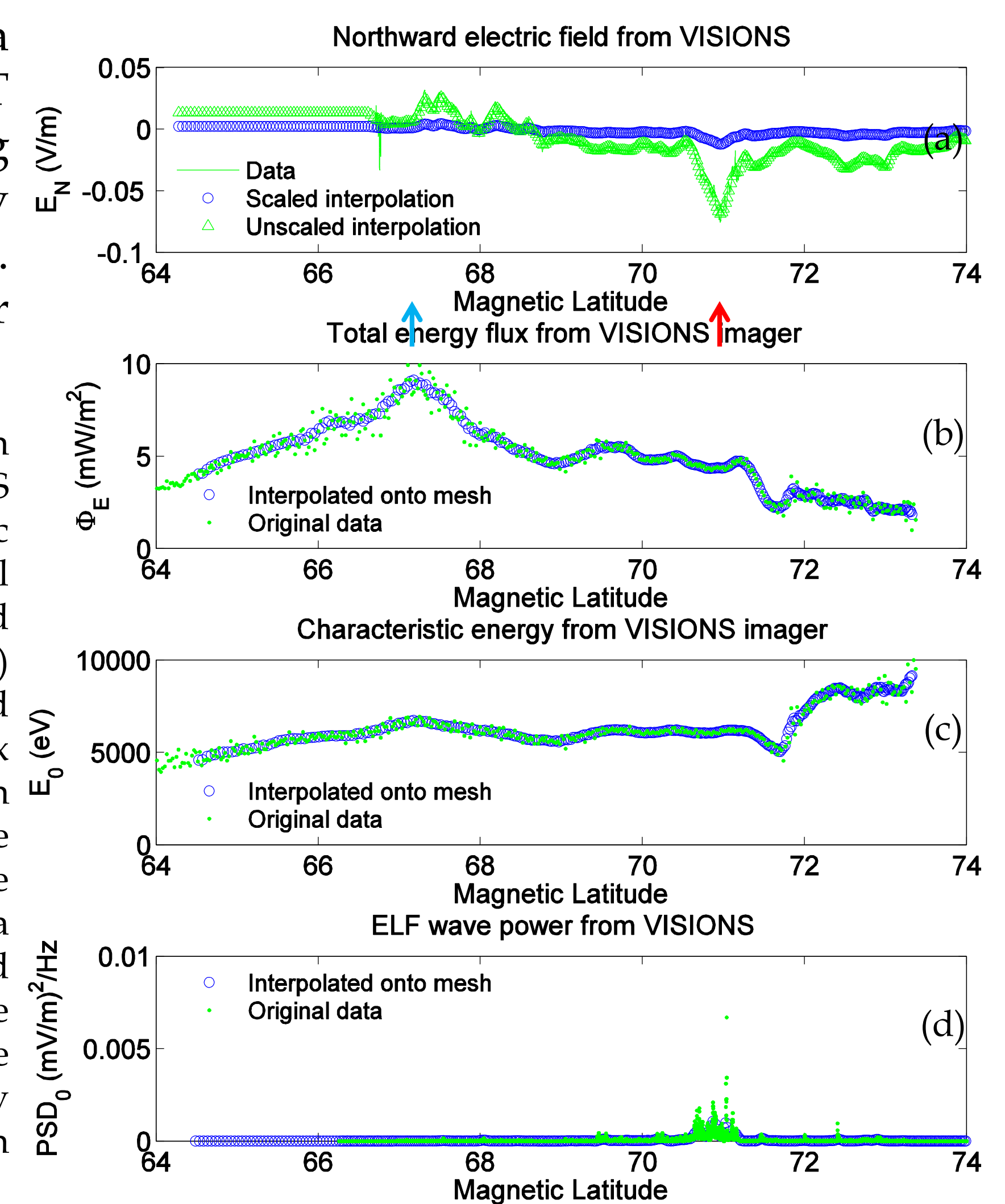


Figure 3: In-situ data is interpolated onto the model's grid providing realistic constraints. Plotted here is the outline of the grid (blue triangles), VISIONS rocket trajectory (black line) traversed right-to-left, PFISR location (pink circle), and the PFISR beam locations (pink dashed-lines).

Figure 4: (Right) In-situ data (green dots or line) collected by the VISIONS sounding rocket, northward electric field (panel a), total energy flux (panel b), characteristic energy (panel c), and the power spectral density (panel d) and interpolated onto the model's grid (blue circles). The total energy flux and characteristic energy have been binned by magnetic latitude. The northward electric field from the rocket trajectory is scaled to be a boundary condition since the field lines get farther apart with altitude but must retain an equipotential. The power spectral density values are very small and not currently included in simulations.



The in-situ data is mapped onto the model's grid and constantly used as ion drivers for the full 200 s of the simulation to generate greater contextual detail of the state of the ionosphere beyond point measurements along the trajectory.

## One Latitude for All Time

Considering a single field line, corresponding to the red arrow in panel a of Figure 4, the local changes in O<sup>+</sup> temperature anisotropy and density over time are plotted below.

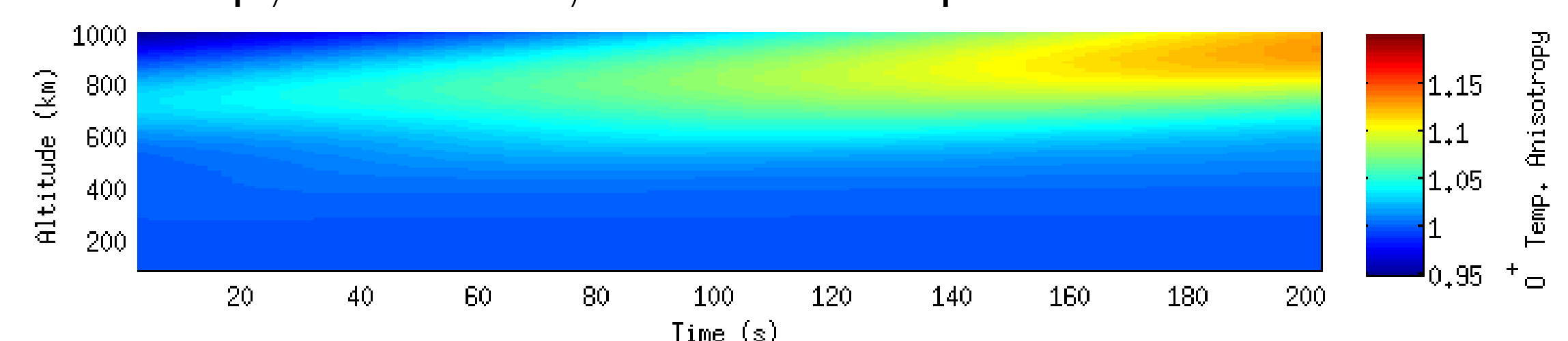
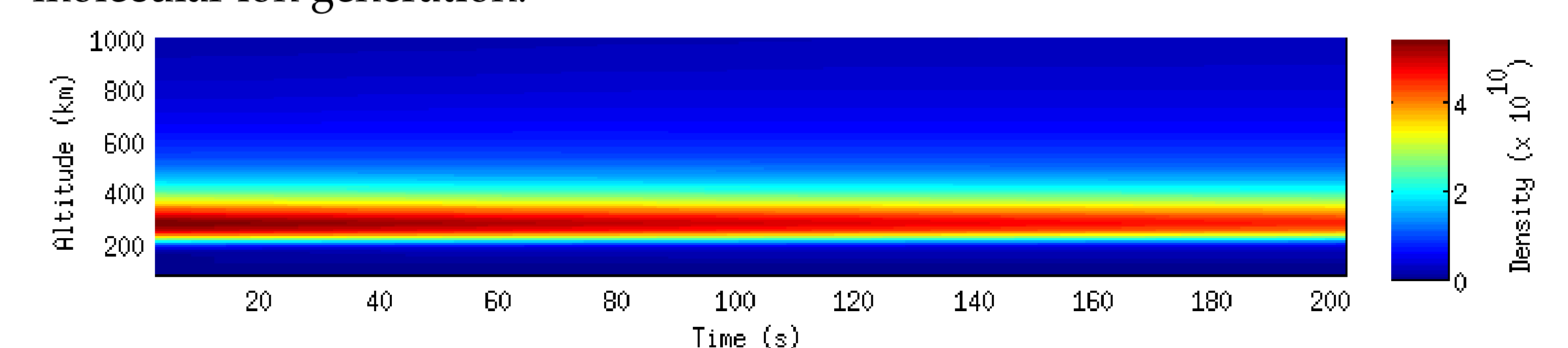


Figure 5: Temperature anisotropies increase over time as the plasma is continuously heated by northward electric fields.

Figure 6: The density changes over time of a single field line from the simulation. The density decreases by 16% over the length of the simulation. DCE can cause density depletions due to enhanced recombination and molecular ion generation.



## All Latitudes at End Time

Considering the full Range, at the end of the simulation, the latitudinal variance in ion response is readily apparent.

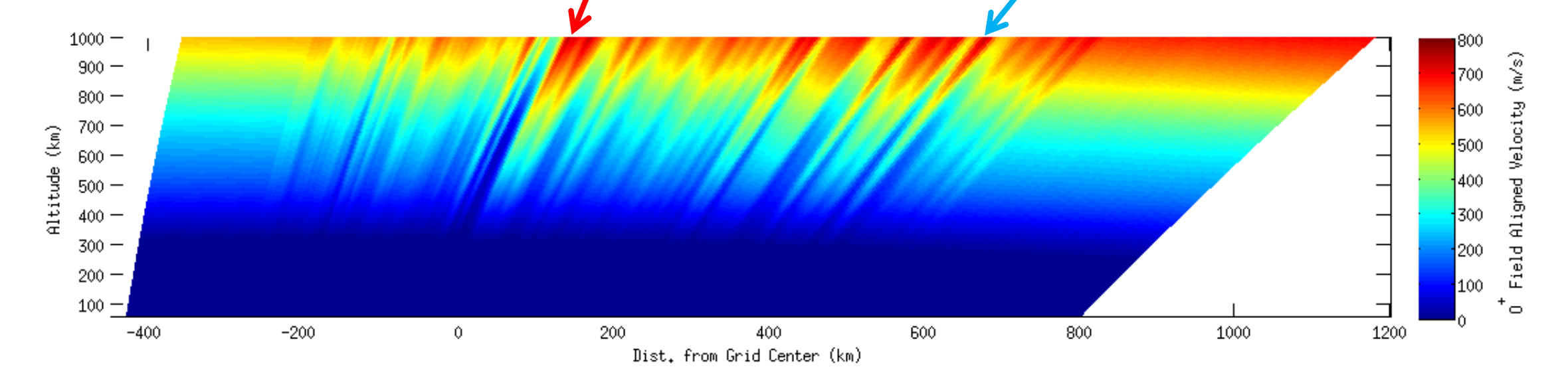
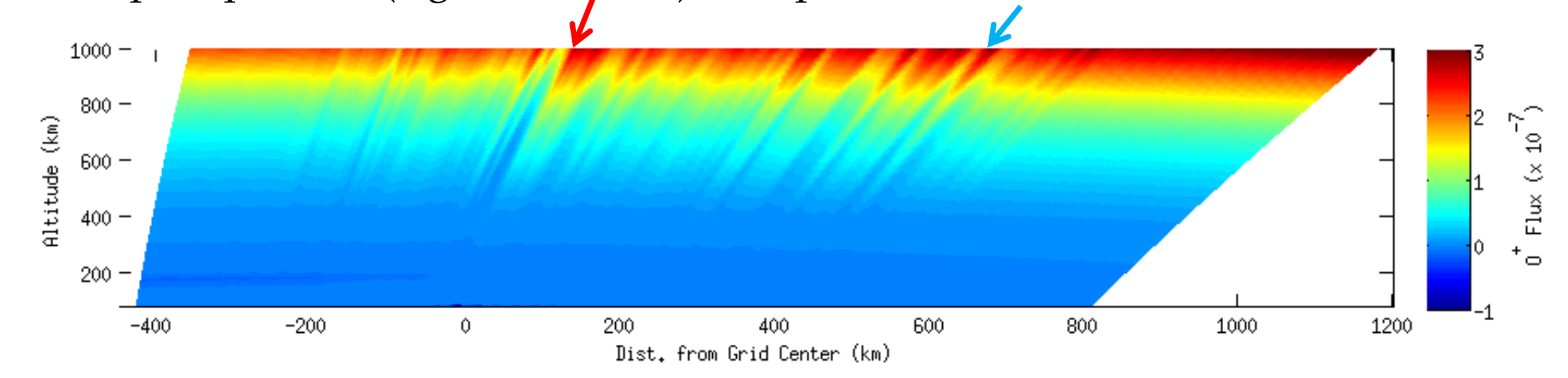


Figure 7: Dynamic O<sup>+</sup> field aligned velocity. Largest upflows correspond to regions of increased DCE (e.g. red arrow) and precipitation (e.g. blue arrow).

Figure 8: The O<sup>+</sup> flux at the end of the simulation. The stronger ion fluxes also correspond to regions of increased northward electric field (e.g. red arrow) and precipitation (e.g. blue arrow) as expected.



## Conclusions & Future Work

- The high-latitude ionosphere is subject to magnetospheric forcing that can result in strong temperature anisotropy and concurrent ion upflow and outflow. An anisotropic model is needed to resolve these temperature anisotropies.
- Perpendicular DC electric fields drive ions through the neutral atmosphere creating frictional heating in addition to expansion and upwelling of plasma. The O<sup>+</sup> flux response to a 80 mV/m DC electric field (DCE) in the isotropic model is 48% larger than in the anisotropic model after 100 s of heating (see Figure 1).
- Wave particle interactions perpendicularly heat ions at higher altitudes providing a secondary energization source feeding ion outflow. Standard reference values for power spectral densities (PSD) create anisotropic temperatures down to ~500 km (blue solid line, Figure 2) but in extreme cases it can be seen down to ~250 km (solid red line, Figure 2).
- Using VISIONS measurements (see Figure 4) to determine the magnitude of the ion drivers, the largest upflows correspond to regions of increased DCE (red arrow, Figure 7) and precipitation (blue arrow, Figure 8). Over the course of the 200 s simulation temperature anisotropies continuously increased in response to the constantly applies heating and the density decreased by 16% due to enhanced recombination and molecular ion generation from DCE (see Figures 5 and 6).
- Future work: Use the total energy flux and characteristic energy from PFISR for a space AND time dependent ion driver.